TRLFS characterization of Eu(III)-doped synthetic organo-hectorite

Nicolas Finck*, Thorsten Stumpf, Clemens Walther, Dirk Bosbach

Institut für Nukleare Entsorgung (INE), Forschungszentrum Karlsruhe, PO Box 3640, D-76021 Karlsruhe, Germany

ARTICLE INFO

Keywords:
Incorporation
Coprecipitation
Europium
Smectite
TRLFS

ABSTRACT

Europium(III) was coprecipitated with the clay mineral hectorite, a magnesian smectite, following a multi-step synthesis procedure. Different Eu(III) species associated with the proceeding synthetic hectorite were characterized by selectively exciting the $^5D_0 \rightarrow {}^7F_0$ transition at low temperature ($T < 20$ K). Fluorescence lifetimes indicated that Eu(III) ions may be incorporated in the octahedral layer of the brucite precursor as well as in the octahedral sheet of the clay mineral. The excitation spectra indicated that the substitution of the divalent Mg by the trivalent Eu induced local structural deformation.

This investigation implements the molecular-level understanding of the *f* element structural incorporation into the octahedral layer of sheet silicates by coprecipitation with clay minerals from salt solutions at 100 °C.

1. Introduction

Clay minerals may play an important role in a high-level nuclear waste (HLW) repository system. Clay-based materials can be used as a backfill or buffer, representing a geotechnical barrier within a multibarrier system (Mallants et al., 2001). Eventually, if the waste matrix gets into contact with ground water, clay minerals may form as secondary phases upon alteration of the waste matrix in the course of the geological evolution of the repository system (Abdelouas et al., 1997; Luckscheiter et al., 2002). For example, the trioctahedral smectite hectorite has been identified in long-term corrosion experiments as one of the secondary phases forming in the alteration layer of HLW glass under near-field conditions (Zwicky et al., 1989).

Many fission products and in particular the actinides (or 5*f* elements) in the HLW have very long half-lives. Consequently, the long-term behaviour of a HLW repository system needs to be considered up to 10^6 years. In particular, the long-term radiotoxicity is solely dominated by the actinides (Salvatores, 2005).

Due to the structural characteristics of clay minerals, several molecular-level binding mechanisms can operate: outer- and inner-sphere surface complexation, cation exchange within the interlayer, and structural incorporation. In addition to adsorption reactions at the external clay mineral surface (including the interlayer), radionuclide (RN) binding by incorporation into the bulk structure of clay minerals may occur via coprecipitation. Trapped in structural sites, RN would be effectively "blocked" from further migration in the geosphere, in particular if a thermodynamically stable solid solution forms. A sound understanding of the molecular-level RN behaviour in the geosphere is required to assess the long-term safety of a HLW repository over geological time spans.

Structural substitution within the tetrahedral and octahedral sheets of various clay minerals in nature has been known for many decades (Brindley and Brown, 1980). In nature, the octahedral layer typically contains cations like Al^{3+}, Fe^{3+}, Fe^{2+}, Mg^{2+}, Mn^{2+} or Ti^{4+} (see for example Dekov et al., 2007, and references therein). Here, we are concerned about the geochemical behaviour of actinides. Several concepts of HLW repository suggest that reducing conditions may prevail: the actinides Am, Cm, and some fractions of Pu may occur in their trivalent redox state. Considering the ionic radii (Shannon, 1976) of cations occupying regular tetrahedral (e.g. ^{IV}Si 0.26 Å) lattice sites in sheet silicates and the ionic radii of trivalent actinide Cm (^{VI}Cm 0.97 Å) a tetrahedral cation substitution can be ruled out. A tetrahedral cation substitution can also be ruled out for the nonradioactive chemical homologue of Cm, the trivalent lanthanide (or 4*f* element) (Chapman and Smellie, 1986) Eu (^{VI}Eu 0.95 Å). The incorporation of *f* elements may

* Corresponding author. Tel.: +49 7247 82 4321; fax: +49 7247 82 3927.
E-mail address: Nicolas.finck@ine.fzk.de (N. Finck).

occur by substitution of ions in the octahedral lattice sites. From a crystal chemistry point of view, they could occupy a 6 fold oxygen coordinated lattice site (Pauling's first rule). However, compared to the size of cations (Shannon, 1976) which typically occur in octahedral sites in sheet silicates (e.g. ^{VI}Al(III) 0.54 Å, ^{VI}Mg(II) 0.72 Å, ^{VI}Li(I) 0.76 Å, ^{VI}Fe(II) 0.78 Å), substitution by trivalent actinides or lanthanides does not seem to be favourable due to the large strain, which would be induced by the substitution of such large cations (Allan et al., 2001).

The formation of sedimentary clay minerals is often deduced from the rare earth elements (REE, or lanthanides) content. The variation in REE concentrations reflects the composition of the fluids from which they precipitated and the structural compatibility for these ions (Severmann et al., 2004). For example, enrichment in heavy (smaller) REE was reported for a hydrothermally formed nontronite, a Fe rich trioctahedral smectite, from the TransAtlantic Geotraverse (TAG) hydrothermal field on the Mid Atlantic Ridge (Severmann et al., 2004), and from Eolo Seamount, Tyrrhenian Sea (Dekov et al., 2007). It was concluded that the REE uptake is controlled by crystal chemistry and that the REE occupy octahedral sites within the clay mineral structure. The Sr isotope data indicate that the clay minerals formed by direct precipitation from the solutions and that the REE were incorporated via coprecipitation. However, no spectroscopic technique was used to directly characterize the incorporated REE species.

Clay minerals containing structurally substituted heavy metal ions have also been synthesized in the laboratory by coprecipitation and by ion exchange (Mn hectorite: Higashi et al., 2007; Zn hectorite: Nakakuki et al., 2004; Ni hectorite: Nakakuki et al., 2005; Tb(III) ion exchange: Lezhnina et al., 2007). Spagnuolo et al. (2004) studied the coprecipitation of transition metal ions during the synthesis of hectorite from aqueous salt solution at 100 °C. Electron paramagnetic resonance (EPR) spectroscopy combined with EDTA extraction experiments indicated that Cu^{2+} (^{VI}Cu 0.73 Å) and Zn^{2+} (^{VI}Zn 0.74 Å) substitute for ions in the octahedral lattice sites more significantly than Cd^{2+} (^{VI}Cd 0.95 Å) and Pb^{2+} (^{VI}Pb 1.19 Å). More than 95% of the total Cu^{2+} and Zn^{2+} concentrations were present within the structure of the coprecipitate, whereas it was about 55 and 30% for Cd^{2+} and Pb^{2+}, respectively.

Tb(III) ion exchange experiments suggested that the lanthanide (^{VI}Tb(III) 0.92 Å; Shannon, 1976) can penetrate into the octahedral sheet of pre existing hectorite (not coprecipitated), based on wet chemical analysis (Lezhnina et al., 2007). However, Miller et al. (1982, 1983) indicated that the migration into the octahedral sites may be relatively restricted for the lanthanides. From the dehydration of exchanged montmorillonite (Yb, Ho and Eu) it was concluded that the migration may occur only at relatively high temperatures.

However, the substitution of cations present in the octahedral layer for the trivalent REE may more likely occur by coprecipitation of clay minerals from solution. Recently, TRLFS investigations on Eu(III) coprecipitation with the magnesian smectite hectorite (Pieper et al., 2006) suggested a trivalent lanthanide incorporation into a solid phase: either in the clay octahedral layer, or in an amorphous silica phase. A TRLFS study on Cm(III) coprecipitation with hectorite strongly indicated an octahedral substitution mechanism (Brandt et al., 2007).

Based on this background, the system Eu/hectorite is used as model system in this study to further investigate the uptake of trivalent REE by coprecipitation with clay minerals. The multi step formation of organo hectorite developed by Carrado et al. (1997a,b, 2000) allows to track the lanthanide through the clay mineral formation. Here we have used low temperature (T<20 K) site selective TRLFS measurements to characterize different Eu(III) species (i.e., a Eu(III) ion in a given chemical environment) during distinct reaction steps on the basis of excitation and emission data.

2. Experimental

2.1. Samples preparation and characterization

Eu(III) containing organo hectorite was synthesized at T≤100 °C following a multi step synthesis procedure (Carrado et al., 1997a,b, 2000). First, a Eu(III) containing $Mg(OH)_2$ precursor was freshly precipitated by dissolving $MgCl_2{\cdot}6H_2O$ (32 mmol, Merck®) in Milli Q water (approximately 400 mL), adding 500 µL of a 1000 µg/mL (3.3×10^{-6} mol) europium solution (Alfa®) (Mg:Eu ~ 9700:1), and by adding a 2 N NH_4OH solution under constant stirring. This brucitic precursor suspension was then centrifuged and washed with 4 volumes of Milli Q water to remove excess ions.

In a 1 l round bottom glass reactor, tetraethylammonium chloride (2.7 mmol, (TEACl), Fluka®) and lithium fluoride (8.5 mmol, Aldrich®) were dissolved in Milli Q water (approximately 400 mL), and the precursor suspension was added. This mixture was constantly stirred using a suspended stirring bar, and brought to reflux in an oil bath. After about 30 min, Ludox HS 30 (48.8 mmol, Sigma Aldrich®), a Na^+ stabilized 30% silica sol, was added drop wise (to reach pH 9 10). The total volume was approximately 500 mL and allowed to react for 8 days. The cooled suspension was centrifuged and the supernatant removed. The synthetic product was treated with HCl Suprapur (Merck®) at pH 3 and 25 °C in order to remove eventual traces from the remaining precursor, and was washed several times with Milli Q water to reach the pH of distilled water. The suspension was filtrated using a 0.05 µm pore diameter filter, washed with Milli Q water, and dried. To this synthesis procedure corresponds a Li:Mg:Si molar ratio of 0.27:1.00:1.52. Assuming a total incorporation of the trivalent lanthanide, this ratio yields the ideal hectorite composition: $Ex_{0.65945}[Li_{0.66}Mg_{5.33945}Eu_{0.00055}Si_8O_{20}(OH/F)_4]$. The corresponding europium content is 100 ppm, which is considered low enough to avoid any possible Eu Eu quenching effect during the TRLFS experiments. However, half of the initially introduced lanthanide may be effectively incorporated, based on previous investigations on Cm(III) ($Mg:Cm=2.3\times10^5:1$) coprecipitation experiments (Brandt et al., 2007).

Separately, a Eu(III) containing precursor ((Mg/Eu) hydroxide) was prepared considering the same Mg:Eu ratio (Mg:Eu ~ 9700:1) as for the clay mineral. This synthesis was carried out under argon atmosphere (glove box) to exclude the formation of aqueous carbonate species. $MgCl_2{\cdot}6H_2O$ (37 mmol, Merck®) was dissolved in Milli Q water (approximately 150 mL) and 580 µL of a 1000 µg/mL (3.8×10^{-6} mol) europium solution (Alfa®) was added. The hydrous compound was precipitated by adding a 2N NH_4OH solution under constant stirring. This suspension was decanted and the supernatant removed. Milli Q water was added and the suspension was stirred; the supernatant was removed after decantation. This

operation was repeated four times to remove excess ions. The dry compound was obtained by freeze drying. The formation of aqueous europium chloride species under these experimental conditions is ruled out based on thermodynamic data. Finally, amorphous europium hydroxide was prepared. Europium oxide (Eu_2O_3, 99.99% purity) was dissolved in 2% perchloric acid and a 2N NH_4OH solution was added drop wise under constant stirring under Ar atmosphere to exclude the formation of carbonate species. This suspension was filtrated and washed with Milli Q water to remove excess ions.

Prior to TRLFS investigations, the Eu(III) doped hectorite and the (Mg/Eu) hydroxide were characterized by X ray diffraction (XRD) and Attenuated Total Reflectance Fourier Transform Infrared (ATR FTIR) spectroscopy. XRD patterns (Brucker® D8 Advance, Cu K_α) were collected from 2° to 60° 2θ, with a step width of 0.02° 2θ. Data (not shown) for the Eu(III) containing hectorite indicated a basal spacing typical for organo hectorite with TEA^+ ions in the interlayer (d_{001} = 14.5 ± 0.3 Å) (Carrado et al., 1997a). This value includes the thickness of the clay layer, which is 9.6 Å for a typical smectite (Grim, 1968). Higher *001* reflections could not be identified. No influence of the coprecipitated lanthanide on the XRD pattern could be observed (peak position and peak intensity). Additionally, the considered substitution degree was too low to have an effect on the XRD pattern. ATR FTIR (Bruker®, IFS 55) spectra were recorded in the range 360 4000 cm^{-1}, collecting 100 scans with a resolution of 2 cm^{-1}. Prior to IR measurements, the chamber was flushed for 2 h with Ar gas to avoid carbon dioxide contamination. Data (not shown) clearly identified the synthetic clay mineral as hectorite. The spectrum displayed OH stretching bands of the Mg_3OH units at 3678 cm^{-1}, and its OH deformation bands at 655 cm^{-1}, combined with the bands associated to the Si O units (990 and 696 cm^{-1}) (Madejovà and Komadel, 2001). All remaining bands of the synthetic clay mineral are in agreement with reported IR spectra of organo hectorite (Carrado et al., 1997a). The strong band characteristic for $Eu(OH)_3$ (3605 cm^{-1}; Farmer, 1974) was not displayed on the Eu(III) containing hectorite spectrum, ruling out its presence in the sample under investigation. The (Mg/Eu) hydroxide was mainly characterized by a band around 3700 cm^{-1} corresponding to the hydroxyl stretching frequency (Brindley and Kao, 1984).

2.2. TRLFS measurements

Time resolved laser fluorescence spectroscopy (TRLFS) has proven to be a versatile tool in Eu(III) speciation studies. The positions of the Eu(III) $^5D_0 \rightarrow {}^7F_J$ ($J = 1$ 4) transitions are almost independent of the chemical environment of the cation. Whereas the intensity of the magnetic dipole (MD) $^5D_0 \rightarrow {}^7F_1$ transition is independent of the chemical environment, the intensity of the induced electric dipole (ED) $^5D_0 \rightarrow {}^7F_2$ transition strongly depends on the local crystal field and local symmetry of the ion (hypersensitive effect) (Jörgensen and Judd, 1964; Carnall et al., 1988). Based on the Judd Ofelt theory, the $^5D_0 \rightarrow {}^7F_0$ transition is both ED and MD forbidden (Judd, 1962; Ofelt, 1962), but is formally allowed only in low symmetry systems.

Further information can be obtained from the lifetime of the probed Eu(III) species, which is a function of the ion environment (complexation, quenching). A linear correlation is observed between the fluorescence intensity decay rate and the number of bound water molecules (O H oscillators) present in the inner coordination sphere (Horrocks and Sudnick, 1979; Kimura and Choppin, 1994; Lis, 2002): efficient energy transfer from the Eu(III) excited state to these ligands results in radiationless deexcitation. Due to the large energy gap between the $^5D_0$ and $^7F_6$ levels (~12,000 cm^{-1}), the $^5D_0$ lifetime of Eu^{3+} in non hydroxo containing inorganic solids is in a few milliseconds range and varies little between 2 K and 300 K. In water, the Eu^{3+} aquo ion is characterized by a lifetime of 110 ± 5 μs, which corresponds to 9 coordinated water molecules. Furthermore, sorbed lanthanide species forming inner sphere surface complexes are usually hydrated by 4 5 water molecules (see for example, Rabung et al., 2000, 2005; Stumpf et al., 2002, 2007; Tertre et al., 2006). Consequently, the lifetime provides direct information about the hydration state of the probed Eu(III) and allows to distinguish between a surface sorbed and an incorporated species. Finally, the number of chemically non equivalent Eu(III) species can be determined by exciting selectively the $^5D_0 \rightarrow {}^7F_0$ transition: since both the ground and the excited states are non degenerated, the number of peak(s) displayed in the spectrum correspond the number of different Eu(III) species.

TRLFS measurements were performed with an excimer pumped dye laser system (Lambda Physics, EMG, 308 nm, Scanmate 2) operating at a frequency of 20 Hz. Direct excitation of the Eu(III) D level was carried out using the dye Coumarin 153 (emission at 522 600 nm), and the dye QUI (emission at 365 404 nm) was used for unselective excitation in the UV range. The Eu(III) fluorescence emission was detected by an optical multichannel system consisting of a Czerny Turner polychromator (Jobin Yvon HR 320) with 300/600/1200 lines/mm gratings and a gated, intensified photodiode array (Spectroscopy Instruments, ST180, IRY 700G). The laser pulse energy was controlled by a pyro electric detector on a pulse to pulse basis. A pulse generator (Spectroscopy Instruments, DG 535) was used to measure the time dependent emission decay. For all measurements, fluorescence line narrowing was not observed.

TRLFS experiments were carried out at T < 20 K because decreasing temperature increases the fluorescence intensity. Cryogenic conditions allow a better spectral resolution of the crystal field splitting of the ^7F_J ($J = 1$ 4) transitions, and a peak (s) narrowing (Albin and Horrocks, 1985) may be expected in the excitation spectra. The cooling system (Cryodyne Cryocooler model 22C, compressor 8200, CTI Cryogenics, USA) used helium as refrigerant and allowed continuous closed cycle cooling of the copper sample holder at the cold head down to T < 20 K in a two stage decompression step. The cold head with the sample holder was surrounded by a vacuum chamber equipped with four quartz glass windows. The pressure at low temperature was in the 10^{-5} 10^{-6} mbar range. An auto tuning controller (model 330 1X, Lake Shore, USA) with a silicon dioxide sensor was used for temperature control. The laser beam was focused on the copper sample holder, and the fluorescence emission signal was collected with a glass fibre and directed onto the polychromator.

Site selective excitation of the $^5D_0 \rightarrow {}^7F_0$ transition experiments were carried out (300 lines/mm grating) from 575.0 to 582.5 or 585.0 nm. For each sample, several excitation wavelengths were considered to record emission spectra, (600

lines/mm grating, resolution ~1 nm (Neon)), and to determine the lifetimes (300 lines/mm grating). The fluorescence lifetimes were determined by varying the delay time between laser pulse and camera gating with time intervals of 20 to 100 μs. The uncertainty associated to the lifetime values was estimated to be ~10%.

Emission spectra were also recorded (600 lines/mm grating, resolution ~1 nm (Neon)) and fluorescence emission lifetimes were determined for unselective excitation at 394 nm (same T and P as previously). The lifetimes were determined by varying the delay time between laser pulse and camera gating with time intervals of 50 to 100 μs (associated uncertainty estimated to ~10%).

3. Results and discussion

The Eu(III) uptake mechanism during the hectorite formation was investigated by TRLFS. The Eu(III) species associated with the (Mg/Eu) hydroxide precursor and the Eu(III) containing organo clay were characterized. These compounds were identified to be key steps for *f* elements incorporation in hectorite via coprecipitation (Brandt et al., 2007). Excitation and emission data are recorded by exciting selectively the $^5D_0 \rightarrow {}^7F_0$ transition to reveal details of the incorporation mechanism.

3.1. (Mg/Eu) hydroxide precursor

The formation of an Eu(III) containing $Mg(OH)_2$ (brucite) precipitate is the first step of the organo hectorite synthesis protocol; it was identified as one of the key steps in the Cm(III) incorporation mechanism (Brandt et al., 2007). The excitation spectrum of the $^5D_0 \rightarrow {}^7F_0$ transition recorded for the (Mg/Eu) hydroxide precursor is presented in Fig. 1A. An intense peak, centered at 579.5 nm, with a full width at half maximum (FWHM) of 2.5 nm is displayed, with a smaller peak at 581.2 nm (FWHM ~ 0.4 nm): the presence of more than one Eu(III) species is evidenced. In order to characterize the different species, emission spectra were recorded and the emission lifetimes of the Eu(III) species were determined for several excitation wavelengths (578.0, 578.5, 579.2, 579.6, 580.2 and 581.2 nm).

Three $^5D_0 \rightarrow {}^7F_J$ ($J = 0, 1, 2$) transitions are displayed in the emission spectra (Fig. 1B). The existence of different species is evidenced by the modification of the spectrum shape with the excitation wavelength.

The observed $^5D_0 \rightarrow {}^7F_0$ transition around 580 nm is in contradiction with the Judd Ofelt theory (Judd, 1962; Ofelt, 1962): it is both ED and MD forbidden. Its presence indicates Eu^{3+} ions with very low site symmetry (C_s, C_n, C_{nv}). The splitting of the $^5D_0 \rightarrow {}^7F_1$ and $^5D_0 \rightarrow {}^7F_2$ emission bands corroborates the low site symmetry around the Eu(III) atoms because of the selection rules for Eu(III) F_J transitions (Görller Walrand et al., 1996). Furthermore, the $^5D_0 \rightarrow {}^7F_2$ / $^5D_0 \rightarrow {}^7F_1$ intensity ratios provide qualitative information on the Eu(III) speciation as a consequence of the hypersensitive effect of the $^5D_0 \rightarrow {}^7F_2$ transition. It varies with the chemical bond and can be considered as an indication of the strength of the ligand field effect. Ratios between 1/8 and 1/4 were reported for the hydrated Eu(III) ions in aqueous solution at pH < 6 (depending on pH, pCO_2, ionic strength, …), between 2/1 and 4/1 for carbonate complexes (depending on pH, pCO_2, ionic strength, …), and 1/1 for hydroxide complexes for 8 < pH < 13 in aqueous solutions (Plancque et al., 2003). For Eu(III) doped solid matrices, values >1 are frequently reported (see for example Babu and Jayasankar, 2000; Venkatramu et al., 2005 and references therein). This ratio is >1 in the (Mg/Eu) hydroxide, what clearly indicates a strong interaction between the probed species and its chemical environment (Fig. 1B).

The fluorescence lifetimes of the Eu(III) species were determined for identical excitation wavelengths (578.0, 578.5, 579.2, 579.6, 580.2 and 581.2 nm). The time dependent emission intensity decays were fitted with multi exponential functions because the presence of more than one species was evidenced. A bi exponential fit describes well the emission decays, considering lifetime values of 350 ± 30 μs and 1700 ± 100 μs. The long lived species (1700 ± 100 μs) corresponds to Eu(III) having lost its entire primary hydration sphere (Horrocks and Sudnick, 1979). The shorter lifetime (350 ± 30 μs) corresponds to Eu(III) bound to 2.5 ± 0.5 H_2O in the inner coordination sphere (Horrocks and Sudnick, 1979). This could also correspond to 5 ± 1 hydroxyl groups, considering the quenching by OH to be half as efficient as quenching by H_2O (Supkowski and Horrocks, 2002). Moreover, the intensity of the fluorescence signal of this latter species indicates that the species with the longer fluorescence lifetime is present only as a minor component (~15% by exciting at 578.0 580.2 nm and ~30% by exciting at 581.2 nm).

3.2. Amorphous europium hydroxide

The (Mg/Eu) hydroxide precursor is precipitated by addition of NH_4OH to an aqueous solution containing Mg(II) and Eu(III) cations up to a pH of 9 10. Under these alkaline conditions, the Eu^{3+} ions are affected by hydrolysis and hydroxide complexes may thus be formed and precipitate. To exclude the formation of such complexes, amorphous europium hydroxide was prepared, washed, dried and immediately analysed without thermal ageing. Consequently, this compound may be amorphous and not crystalline. A single peak (centred at 579.6 nm, FWHM 1.6 nm) is present in the excitation spectrum (Fig. 2A). The emission spectra collected for different excitation wavelengths (578.0, 578.4, 579.6 and 580.3 nm) are identical (Fig. 2B), and the time dependent intensity decays were successfully fitted by mono exponential functions (lifetime 230 ± 20 μs). These data are consistent with the presence of a unique Eu(III) species. The lifetime value indicates 4.0 ± 0.5 H_2O molecules bound to Eu(III) in the primary hydration sphere (Horrocks and Sudnick, 1979), corresponding to 8 ± 1 hydroxyl groups (Supkowski and Horrocks, 2002). This lifetime is significantly shorter than what we found in the case of the (Mg/Eu) hydroxide, even for the short component. This is in agreement with X ray diffraction (Mullica et al., 1979) and EXAFS (Schlegel et al., 2004) data indicating that Eu(III) is bound to 9 oxygens. This result rules out the formation of an amorphous europium hydroxide compound as a secondary phase during the (Mg/Eu) hydroxide precursor synthesis.

3.3. Eu(III) doped organo hectorite

Ageing the (Mg/Eu) hydroxide precursor in the presence of silica completes the clay synthesis. The condensation of the silica tetrahedral sheet onto the precursor was identified as

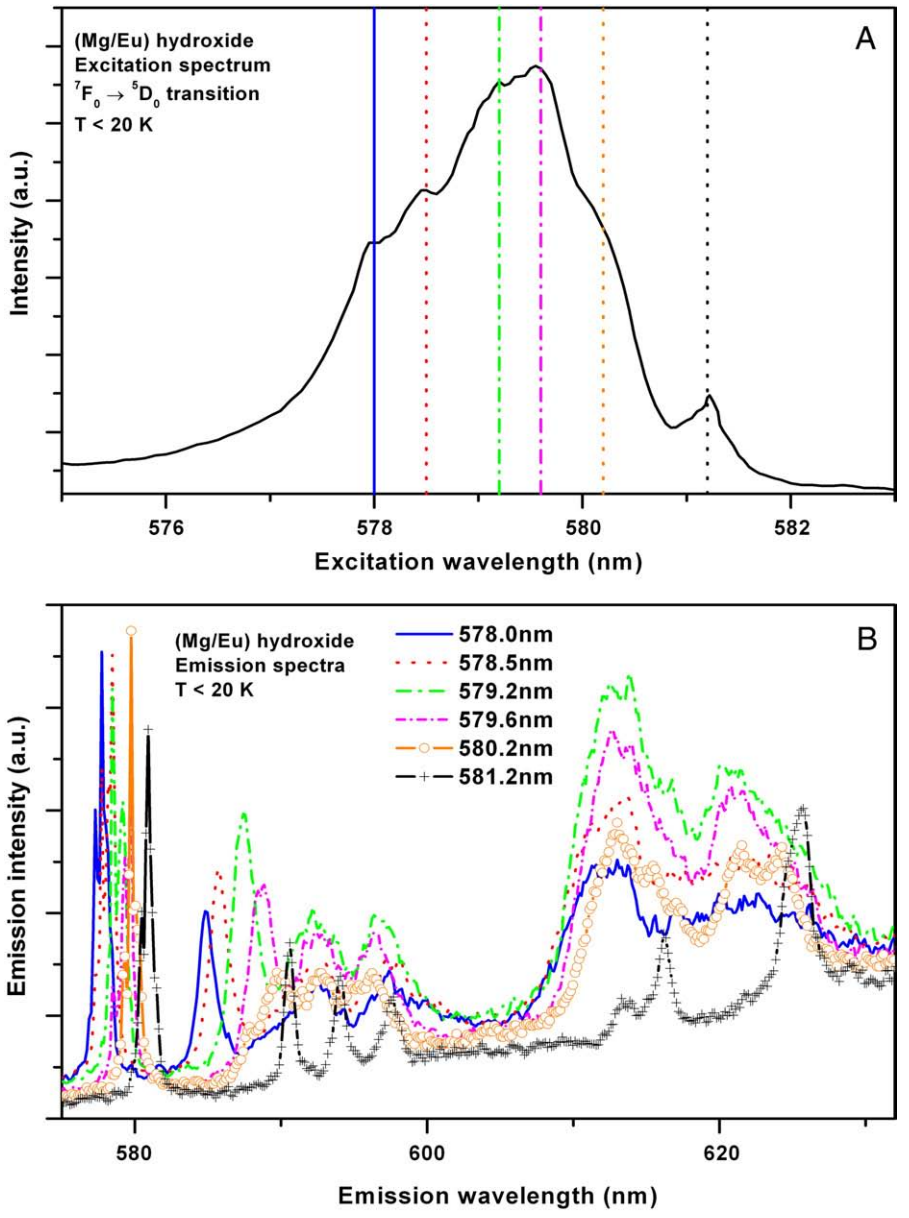

Fig. 1. Excitation (A) and emission (B) spectra for the (Mg/Eu) hydroxide precursor. The emission spectrum shape is modified with the excitation wavelength, evidencing the presence of more than one Eu(III) species.

the second key step in the Cm(III) coprecipitation with hectorite (Brandt et al., 2007). Fig. 3A shows the excitation spectrum of the $^5D_0 \rightarrow {}^7F_0$ transition recorded for the Eu(III) containing organo hectorite: a single intense peak (FWHM 2 nm) centred at 579.4 nm is displayed. Considering the FWHM of the peak (FWHM 2.5 nm) obtained previously for the (Mg/Eu) hydroxide (Fig. 1A), different species may be convoluted in this signal. Emission data were recorded for different excitation wavelengths (578.3, 579.0, 579.4 and 580.0 nm) to clarify this point.

Three $^5D_0 \rightarrow {}^7F_J$ (J=0, 1, 2) transitions are displayed in the emission spectra (Fig. 3B). The spectrum shape modification with the excitation wavelength indicates the presence of a suite of coordination environments, resulting in the observed band shift.

As for the precursor, the presence of the $^5D_0 \rightarrow {}^7F_0$ transition and the splitting of the $^5D_0 \rightarrow {}^7F_J$ (J=1, 2) emission bands indicate a low site symmetry (C_s, C_n, C_{nv}) (Görller Walrand and Binnemans, 1996). The intensity decrease of the $^5D_0 \rightarrow {}^7F_0$ transition as the excitation wavelength is varied from 578.3 to 580.0 nm further evidences the presence of more than one Eu (III) species. Finally, the $^5D_0 \rightarrow {}^7F_2$ / $^5D_0 \rightarrow {}^7F_1$ intensity ratio (>1) indicates a strong interaction between the probed Eu(III) and its chemical environment.

The fluorescence lifetimes of the Eu(III) species were determined for identical excitation wavelengths (578.3, 579.0,

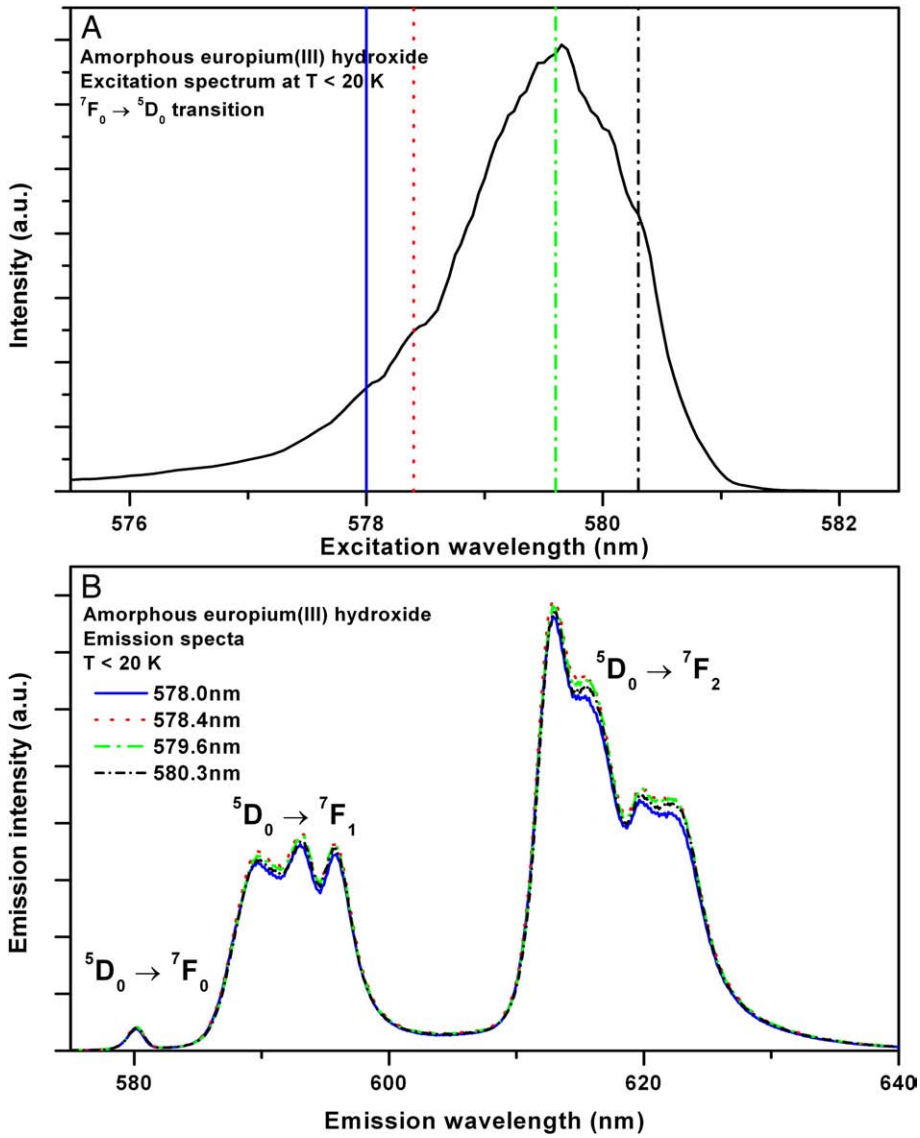

Fig. 2. Excitation (A) and emission (B) spectra for the amorphous Eu(III) hydroxide compound. The emission spectrum shape is not modified with the excitation wavelength, contrarily to the (Mg/Eu) hydroxide compound: only one species may be present.

579.4 and 580.0 nm). The emission signal data were fitted with multi exponential functions for all excitation wave lengths because the presence of more than one species was evidenced. A bi exponential fit describes well the emission decays, considering lifetime values of 580±50 μs and 1890± 100 μs. The long lived species corresponds to Eu(III) having lost its entire primary hydration sphere (Horrocks and Sudnick, 1979). The second lifetime value (580±50 μs) cha racterizes a species having 1.0±0.5 H_2O in the inner coor dination sphere, which could also correspond to 2±1 hydroxyl groups (Supkowski and Horrocks, 2002). The intensity of the fluorescence signal of this second species indicates that the long lived species is not present as the major component (Table 2, Fig. 4.).

Low temperature TRLFS experiments were then carried out by exciting Eu(III) to the $^5L_6$ level (excitation wavelength 394.0 nm) instead of selectively exciting to the $^5D_0$ level. The emission spectrum appeared noisy. However, the $^5D_0 \rightarrow {}^7F_2$ / $^5D_0 \rightarrow {}^7F_1$ intensity ratio is >1 and the determined lifetime values are the same as those obtained for selective excitation (Table 2).

3.4. Discussion

Molecular level information about the Eu(III) uptake mechanism by coprecipitation with hectorite was obtained by collecting low temperature (T<20 K) site selective TRLFS data. However, the characterization of the Eu(III) species associated with the stepwise clay mineral synthesis may only be pertinent if the clay formation mechanism is known. First, the crystallization of the pure organo hectorite was investi gated in detail by Carrado et al. (1997a,b). Secondly, in the study of physicochemical sequestration of transition metal

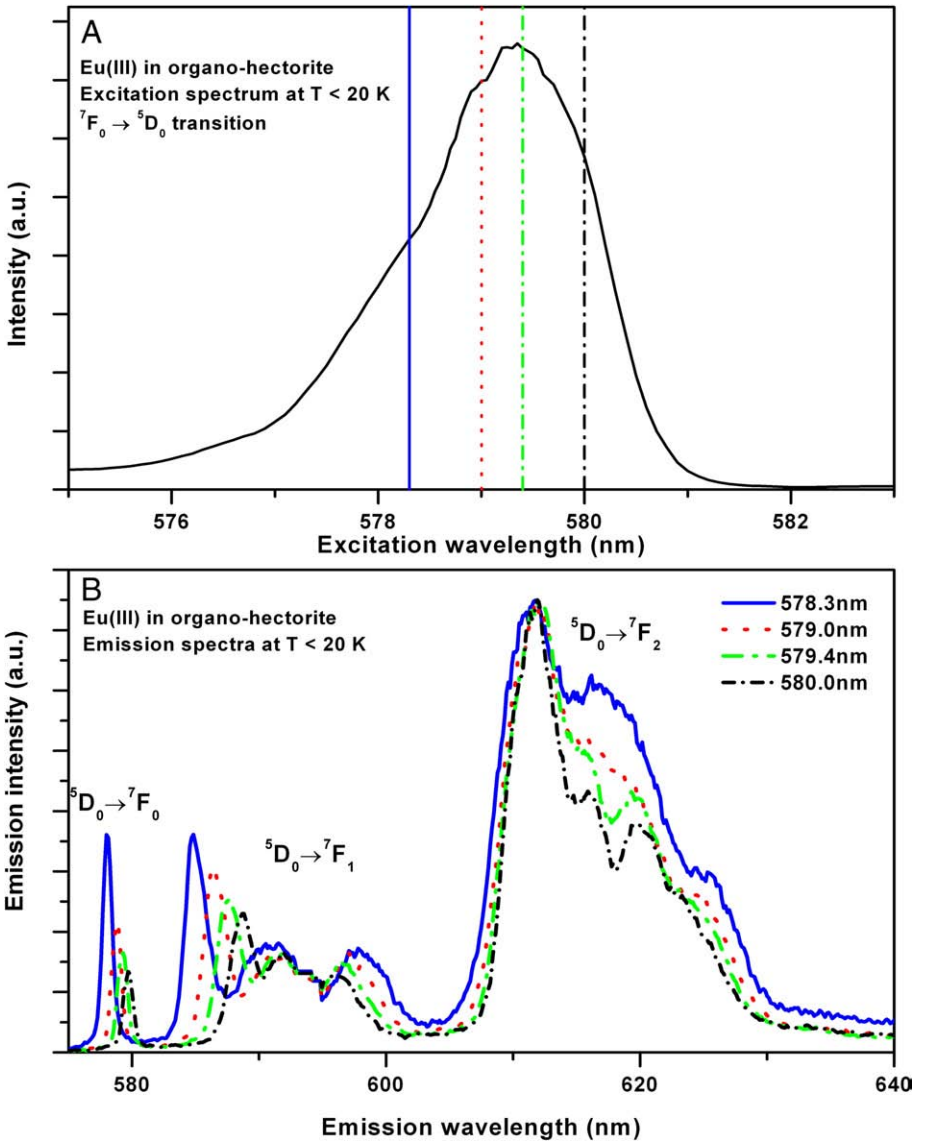

Fig. 3. Excitation (A) and emission (B) spectra for the Eu(III)-doped organo-hectorite. The emission spectrum shape is gradually modified with the excitation wavelength, evidencing the presence of more than one Eu(III) species.

ions, low levels of metal ions (Cd^{2+}, Pb^{2+}, Cu^{2+} and Zn^{2+}) in hydrothermally coprecipitated hectorites were found to have no effect on the formation or degree of crystallinity of the synthetic clays, as revealed by FTIR and XRD data (Spagnuolo et al., 2004). Also, no significant influence on the hectorite or its morphology by the coprecipitation of trivalent *f* elements was evidenced based on XRD and FTIR data combined with SEM and AFM images (Pieper et al., 2006; Brandt et al., 2007). The modified precursor was assumed to induce no significant change in the established organo hectorite formation mechanism used for the Eu(III)/Cm(III) TRLFS data interpretation (Pieper et al., 2006; Brandt et al., 2007). In the present investigation also, no significant influence of the coprecipitation of Eu(III) on the clay mineral structure could be observed.

The excitation spectra collected by selectively exciting the $^5D_0 \rightarrow {}^7F_0$ transition at T<20 K, for both the (Mg/Eu) hydroxide and the Eu(III) doped organo hectorite, contain an intense peak of similar FWHM, and a second smaller peak is observed for the doped brucite compound (Table 1). The broad peaks can hardly be explained by only one Eu(III) species. They are broad compared to reported experimental data for Eu(III) doped hydrotalcite (FWHM ~ 1.4 nm; Stumpf et al., 2007), calcite (FWHM < 0.4 nm; Marques Fernandes et al., in press) or strontium fluorophosphates (FWHM ~ 0.4 nm; Wright et al., 1995). The data collected in this study may compare with values reported for Eu^{3+} doping lead borate glass (FWHM ~ 1.8 nm; Venkatramu et al., 2005) or fluoroborate glass (FWHM ~ 2.1 nm; Lavín et al., 2001). For these two glasses, it was concluded that the linewidth of the band was associated to the large distribution of environments and/or sites possible for the Eu (III) ions in the matrices. In the (Mg/Eu) hydroxide and in the Eu (III) doped organo hectorite, the trivalent lanthanide may

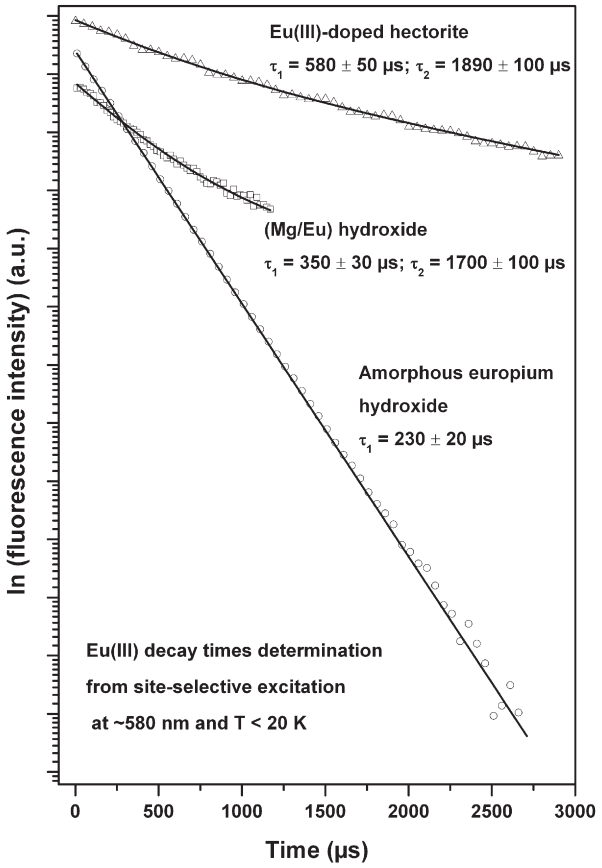

Fig. 4. Fitting of the fluorescence decay for the three compounds under investigation for an excitation wavelength of ~580 nm.

substitute the divalent magnesium at the octahedral lattice site. This substitution may induce a lattice distortion. The charge compensation can be realized by cations present in the interlayer or at the surface. The substitution of divalent Mg cations by monovalent Li ions in the octahedral layer can also achieve the charge compensation. Consequently, the substitution mechanism may induce a large distribution of environments for the Eu(III) ions which could explain the rather large FWHM of the dominating peak in the excitation spectra (Figs. 1A and 3A).

The modification of the emission spectrum shape with the excitation wavelength evidences the simultaneous presence of more than one species in both compounds (Figs. 1B and 3B). The associated fluorescence decays follow bi-exponential functions. A long-lived species is evidenced for both samples: 1700±100 μs for the precursor and 1890±100 μs for the organo-clay. These values correspond to a complete loss of water molecules present in the first coordination sphere of the lanthanide ion (Horrocks and Sudnick, 1979). However, these species are only present as a minor component (Table 2).

The short-lived species (main component; 350±30 μs) detected in the (Mg/Eu) hydroxide indicates the presence of 2.5±0.5 H_2O (Horrocks and Sudnick, 1979) or 5±1 OH-groups (Supkowski and Horrocks, 2002) in the first coordination shell of the Eu(III) ions. This species can correspond either to a surface complex, or to an incorporated species in a nearly octahedral environment. In brucite ($Mg(OH)_2$), the magnesium atom is in the centre of an octahedron of hydroxyls. Taking the strong ligand field (Fig. 1B) and the fluorescence lifetime into account, this species may correspond to Eu(III) ion that is incorporated into the brucite lattice. The lanthanide ion surrounded by six hydroxyl groups may approximately replace Mg^{2+} in the brucite octahedral sheet. This result agrees with TRLFS investigations on the Cm(III) coprecipitation with hectorite (Brandt et al., 2007). It was concluded that the actinide is structurally incorporated in a brucite-like (Mg, Cm) hydroxide. The Eu^{3+} incorporation into the brucite octahedral sheet is also supported by the study of the Eu(III) incorporation into hydrotalcite, a brucite-like compound (Stumpf et al., 2007). TRLFS data combined with X-ray absorption spectroscopy (XAS) indicated that Eu(III) is incorporated into the bulk structure, and that the incorporated species induces lattice distortion. Nevertheless, the possibility of a surface complex cannot be totally excluded. However, a value of 4–5 water molecules in the first coordination sphere is usually found for lanthanide and actinide surface complexes. Taking the lifetime value (350±30 μs) into account, the hypothesis of a Eu(III) surface complex can be excluded.

The short-lived species (580±50 μs) detected in the doped organo-clay indicates the presence of 1.0±0.5 H_2O (Horrocks and Sudnick, 1979) or 2±1 OH-groups (Supkowski and Horrocks, 2002) in the Eu(III) first coordination shell. Obviously, water molecules were released from the forming hectorite as a consequence of the condensation of $[SiO_4]$-tetrahedra onto the pre-existing precursor to complete the clay mineral synthesis (Carrado et al., 1997a,b). Taking the lifetime into account, this species may not be surface-sorbed since a value of 4–5 water molecules is usually found for lanthanide and actinide surface complexes. Furthermore, a lifetime value of 284 μs was reported for Eu(III) sorbed onto hectorite (Pieper et al., 2006). This lifetime is significantly shorter as the value obtained in the present study.

The basic structural unit of hectorite consists of one sheet of edge-sharing $[Mg/Li(O,OH)_6]$-octahedra sandwiched between two sheets of corner-sharing $[SiO_4]$-tetrahedra. All octahedral sites are occupied by Mg(II). The unshared $[SiO_4]$-tetrahedra apices point in the direction of the $[Mg/Li(O,OH)_6]$-octahedral sheet and connect the three sheets to the common TOT structure of 2:1 sheet silicates. Substitution of Mg(II) by Li(I) in the octahedral sheet leads to a negative charge. The

Table 1
Characteristics of the Eu(III) site-selective excitation data

Eu(III) compound	Peak position (nm)	Peak FWHM (nm)	Comment
Amorphous Eu(III) hydroxide	579.6	1.6	Single Eu(III) species
(Mg/Eu) hydroxide	579.5	2.5	Excitation bands overlap
	581.2	0.4	
Eu(III)-doped organo-hectorite	579.4	2.0	Excitation bands overlap

Table 2
Fluorescence emission characteristics for several Eu(III) species/compounds

Eu(III) species/compound	$^5D_0 \rightarrow {}^7F_2/{}^5D_0 \rightarrow {}^7F_1$ intensity ratios	Decay times (μs)	Proportion	Comment
Eu^{3+}_{aquo} ions	1/8–1/4 (Plancque et al., 2003)	110 (±5)	100	9 H_2O (Horrocks and Sudnick, 1979)
Amorphous Eu(III) hydroxide	~2/1	230 (±20)	100	4 H_2O/8 OH^-
(Mg/Eu) hydroxide	~2/1	350 (± 30)	85	2.5 H_2O/5 OH^- [a]
		1700 (±100)	15	0 H_2O/OH^- [b]
Eu(III)-doped hectorite	~3/1	580 (±50)	55–65	1 H_2O/2 OH^- [c]
		1890 (±100)	35–45	0 H_2O/OH^- [b]

The fitting of the fluorescence decay profiles at excitation wavelength of ~580 nm are presented in Fig. 4.
Uncertainties are ±0.5 H_2O/±1 OH^-. $^5D_0 \rightarrow {}^7F_1/{}^5D_0 \rightarrow {}^7F_2$ intensity ratios determined at excitation wavelength of ~580 nm.
[a] Eu(III) in a brucite octahedral.
[b] Dehydrated Eu(III) species.
[c] Eu(III) in a clay octahedral environment.

negatively charged TOT layers are linked by exchangeable cations (Breu et al., 2003; Meunier, 2005). Based on the lifetime value, the 2±1 OH^- quenchers present in the first Eu(III) coordination sphere are in accordance with the two OH groups at the unconnected corners of the $[Mg/Li/Eu(O/OH)_6]$ octahedra in the octahedral layer. Consequently, this indicates that the lanthanide substitutes for the cations present at the octahedral lattice site. Again, this result agrees with TRLFS investigations on the Cm(III) coprecipitation with hectorite (Brandt et al., 2007). Data indicated that the actinide is structurally incorporated in the hectorite like TOT layers.

An important structural consequence of the condensation of the tetrahedral sheets onto the pre existing (Mg/Eu) hydroxide precursor is a change in the distance between adjacent octahedral sites. The spacing changes from 3.14 Å in brucite (Zigan and Rothbauer, 1967) to 3.03 Å in hectorite (Breu et al., 2003). The distances are not known for Eu(III) substituting for Mg(II), but are supposed to follow the same trend. Consequently, the structure is denser in the clay as in the brucite, what may affect the Eu ligand field. This is evidenced by the corresponding $^5D_0 \rightarrow {}^7F_2$ / $^5D_0 \rightarrow {}^7F_1$ intensity ratios (Table 2).

4. Conclusion

This TRLFS investigation shows that the trivalent lanthanide europium can be structurally incorporated into the octahedral sheet of hectorite via coprecipitation. This result is in agreement with previous Eu(III)/Cm(III) coprecipitation experiments (Pieper et al., 2006; Brandt et al., 2007). The results of this investigation will be confirmed by a XAS study, as measurements at the Eu L_{III} edge will enable to probe the local environment around the Eu cations in more detail (interatomic distances and coordination numbers).

TRLFS data indicate that the geometric configuration of the hectorite lattice site is flexible enough to accommodate the larger europium, with different charge and ionic radius, as compared to Mg(II). However, due to its size, the structural compatibility of octahedrally coordinated Eu(III) in hectorite may be limited. Nevertheless, since the Cm(III) incorporation into the hectorite octahedral sheet has been demonstrated (Brandt et al., 2007), and based on the present study, it can be concluded that the same mechanism applies for other trivalent *f* elements (Am, Pu, REE). It can also be hypothesized that the incorporation of these elements in an octahedral sheet with 6 fold oxygen coordination may be applicable to other clay minerals/sheet silicates. Nevertheless, this investigation does not allow to conclude about the thermodynamic stability of the *f* element doped clay mineral. However, it might be stable, at least under certain geochemical conditions, since Eu(III)/Cm(III) remains in the clay structure, and because smectites in natural sediments seem to contain structurally incorporated REE (Uysal and Golding, 2003; Severmann et al., 2004; Dekov et al., 2007).

This study has added to the molecular level understanding of *f* element binding mechanisms to clay minerals in aqueous systems. The neoformation of clay minerals by reaction of water with minerals opens the possibility to structurally incorporate RN by coprecipitation. The RN present in solution may be efficiently immobilized by this binding mechanism. However, "colloidal" clay particles may also play a carrier role for actinide migration in natural aquifer systems.

Acknowledgements

N.F. gratefully acknowledges the financial support of the Network of Excellence Actinet. Many thanks to S. Büchner and M. Schmidt (Forschungszentrum Karlsruhe, INE) for their assistance during the TRLFS measurements, and S. Heck for her help in the laboratory. This work was co financed by the Helmholtz Gemeinschaft Deutscher Forschungszentren (HGF) by supporting the Helmholtz Hochschul Nachwuchsgruppe "Aufklärung Geochemischer Reaktionsmechanismen an der Wasser/Mineralphasen Grenzfläche".

References

Abdelouas, A., Crovisier, J.L., Lutze, W., Grambow, B., Dran, J.C., Müller, R., 1997. Surface layers on a borosilicate nuclear waste glass corroded in $MgCl_2$solution. J. Nucl. Mater. 240 (2), 100–111.
Albin, M., Horrocks Jr., W.D.e.W., 1985. Europium(III) luminescence excitation spectroscopy. Quantitative correlation between the total charge on the ligands of the $^7F_0 \rightarrow {}^5D_0$ transition frequency in europium(III) complexes. Inorg. Chem. 24, 895–900.
Allan, N.L., Blundy, J.D., Purton, J.A., Lavrentiev, M.Y., Wood, B.J., 2001. Trace element incorporation in minerals and melts. In: Geiger, C.A. (Ed.), EMU Notes in Mineralogy, Vol. 3: Solid Solutions in Silicates and Oxides Systems. Eötvös University Press, Budapest.
Babu, P., Jayasankar, C.K., 2000. Optical spectroscopy of Eu^{3+} ions in lithium borate and lithium fluoroborate glasses. Physica. B 279, 262–281.
Brandt, H., Bosbach, D., Panak, P.J., Fanghänel, T., 2007. Structural incorporation of Cm(III) in trioctahedral smectite hectorite: a time-resolved laser fluorescence spectroscopy (TRLFS) study. Geochim. Cosmochim. Acta 71 (1), 145–154.
Breu, J., Seidl, W., Stoll, A., 2003. Disorder in smectites in dependence of the interlayer cation. Z. Allg. Anorg. Chem. 629, 503–515.
Brindley, G.W., Brown, G., 1980. Crystal Structures of Clay Minerals and their X-ray Identification. Mineralogical Society, London.

Brindley, G.W., Kao, C.C., 1984. Structural and IR relations among brucite-like divalent metal hydroxides. Phys. Chem. Miner. 10 (4), 187–191.

Carnall, W.T., Goodman, G.L., Rajnak, K., Rana, R.S., 1988. A systematic analysis of the spectra of the lanthanides doped into single crystals LaF_3. Report ANL-88-8. Argonne National Laboratory, Argonne, IL.

Carrado, K.A., Thiyagaraja, P., Song, K., 1997a. A study of organo-clay crystallization. Clay Miner. 32, 29–40.

Carrado, K.A., Zajac, G.W., Song, K., Brenner, J.R., 1997b. Crystal growth of organohectorite clay as revealed by atomic force microscopy. Langmuir 13, 2895–2902.

Carrado, K.A., Xu, L., Gregory, D.M., Song, K., Seifert, S., Botto, R.E., 2000. Crystallization of a layered silicate clay as monitored by small-angle X-ray scattering and NMR. Chem. Mater. 12, 3052–3059.

Chapman, N.A., Smellie, J.A.T., 1986. Introduction and summary of the workshop: natural analogues to the conditions around a final repository for high-level radioactive waste. Chem. Geol. 55, 167–173.

Dekov, V.M., Kamenov, G.D., Stummeyer, J., Thiry, M., Savelli, C., Shanks, W.C., Fortin, D., Kuzmann, E., Vértes, A., 2007. Hydrothermal nontronite formation at Eolo Seamount (Aeolian volcanic arc Tyrrhenian Sea). Chem. Geol. 245, 103–119.

Farmer, V.C., 1974. Infrared spectra of minerals. In: Farmer, V.C. (Ed.), Mineralogical Society Monograph 4. Mineralogical Society, London.

Görller-Walrand, C., Binnemans, K., 1996. Rationalization of crystal-field parametrization. In: Gschneider, K.A., Eyring, L. (Eds.), Handbook on the Physics and Chemistry of Rare Earths, vol. 23. Elsevier, Amsterdam. Chap. 155.

Grim, R.E., 1968. Clay Mineralogy. McGraw-Hill, New York.

Higashi, S., Miki, H., Komarneni, S., 2007. Mn-smectites: hydrothermal synthesis and characterization, Appl. Clay Sci., 38 (1–2), 104–112.

Horrocks Jr., W.D.e.W., Sudnick, D.R., 1979. Lanthanides ion probes of structure in biology. Laser induced luminescence decay constants provide a direct measure of the number of metal-coordinated water molecules. J. Am. Chem. Soc. 101 (2), 334–340.

Jörgensen, C.K., Judd, B.R., 1964. Hypersensitive pseudo-quadrupole transitions in lanthanides. Mol. Phys. 8, 281–290.

Judd, B.R., 1962. Optical absorption intensities of rare earth ions. Phys. Rev. 127 (3), 750–761.

Kimura, T., Choppin, G.R., 1994. Luminescence study on determination of the hydration number of Cm(III). J. Alloys Compd. 213–214, 313–317.

Lavín, V., Babu, P., Jayasankar, C.K., Martín, I.R., Rodríguez, V.D., 2001. On the local structure of Eu^{3+} ions in oxyfluoride glasses. Comparison with fluoride and oxide glasses. J. Chem. Phys. 115 (23), 10935–10944.

Lezhnina, M., Benavente, E., Bentlage, M., Echevarría, Y., Klumpp, E., Kynast, U., 2007. Luminescent hybrid material based on a clay mineral. Chem. Miner. 19, 1098–1102.

Lis, S., 2002. Luminescence spectroscopy of lanthanide(III) ions in solution. J. Alloys Compd. 341, 45–50.

Luckscheiter, B., Nesovic, M., 2002. Sorption behavior of Am on precorroded HLW glass in water and brine. Radiochim. Acta 90, 537–541.

Madejovà, J., Komadel, P., 2001. Baseline studies of the Clay Minerals Society source clays: infrared methods. Clays Clay Miner. 49 (5), 410–432.

Mallants, D., Marivoet, J., Sillen, X., 2001. Performance assessment of the disposal of vitrified high-level waste in a clay layer. J. Nucl. Mater. 298 (1–2), 125–135.

Q2 Marques Fernandes, M., Schmidt, M., Stumpf, T., Walther, C., Bosbach, D., Klenze, R., and Fanghänel, T., in press. Site-selective time resolved laser fluorescence spectroscopy of Eu3+ doped calcite. J. Colloid Interface Sci.

Meunier, A., 2005. Clays. Springer, Berlin – Heidelberg.

Miller, S.E., Heath, G.R., Gonzalez, R.D., 1982. Effect of temperature on the sorption of lanthanides by montmorillonite. Clays Clay Miner. 30 (2), 111–122.

Miller, S.E., Heath, G.R., Gonzalez, R.D., 1983. Effect on pressure on the sorption of Yb by montmorillonite. Clays Clay Miner. 31 (1), 17–21.

Mullica, D.F., Milligan, W.O., Beall, G.W., 1979. Crystal structures of $Pr(OH)_3$, $Eu(OH)_3$, and $Tm(OH)_3$. J. Inorg. Nucl. Chem. 41, 525–532.

Nakakuki, T., Fujimura, K., Aisawa, S., Hirahara, H., Narita, E., 2004. Synthesis and physicochemical properties of Zn-hectorite. Clay Sci. 12, 285–291.

Nakakuki, T., Hirahara, H., Aisawa, S., Takahashi, S., Narita, E., 2005. Hydrothermal synthesis and physiochemical properties of Ni-hectorite. Clay Sci. 13, 19–26.

Ofelt, G.S., 1962. Intensities of crystal spectra of rare-earths ions. J. Chem. Phys. 37 (3), 511–520.

Pieper, H., Bosbach, D., Panak, P.J., Rabung, T., Fanghänel, T., 2006. Eu(III) coprecipitation with the trioctahedral clay mineral, hectorite. Clays Clay Miner. 54 (1), 47–55.

Plancque, G., Moulin, V., Toulhoat, P., Moulin, C., 2003. Europium speciation by time-resolved laser-induced fluorescence. Anal. Chim. Acta 1, 11–22.

Rabung, T., Stumpf, T., Geckeis, H., Klenze, R., Kim, J.I., 2000. Sorption of Am (III) and Eu(III) onto γ-alumina: experiment and modelling. Radiochim. Acta 88, 711–716.

Rabung, T., Pierret, M.C., Bauer, A., Geckeis, H., Bradburry, M.H., Baeyens, B., 2005. Sorption of Eu(III)/Cm(III) on Ca-montmorillonite and Na-illite. Part 1: batch sorption and time-resolved laser fluorescence spectroscopy experiments. Geochim. Cosmochim. Acta 69 (23), 5393–5402.

Salvatores, M., 2005. Nuclear fuel strategies including partitioning and transmutation. Nucl. Eng. Des. 235, 805–816.

Schlegel, M.L., Pointeau, I., Coreau, N., Reiller, P., 2004. Mechanism of europium retention by calcium silicate hydrates: an EXAFS study. Environ. Sci. Technol. 38 (16), 4423–4431.

Severmann, S., Mill, R.A., Palmer, M.R., Fallick, A.E., 2004. The origin of clay minerals in active and relict hydrothermal deposits. Geochim. Cosmochim. Acta 68, 73–88.

Shannon, R.D., 1976. Revised effective ionic radii and systematic studies of interatomic distances in halides and chalcogenides. Acta Crystallogr., A 32, 751–767.

Spagnuolo, M., Martinez, C.E., Jacobson, A.R., Baveye, P., McBride, M.B., Newton, J., 2004. Coprecipitation of trace metal ions during synthesis of hectorite. Appl. Clay Sci. 27, 129–140.

Stumpf, T., Bauer, A., Coppin, F., Fanghänel, T.h., Kim, J.I., 2002. Inner-sphere, outer-sphere and ternary surface complexes: a TRLFS study of the sorption process of Eu(III) onto smectite and kaolinite. Radiochim. Acta 90, 345–349.

Stumpf, T., Curtius, H., Walther, C., Dardenne, K., Ufer, F., Fanghänel, T., 2007. Incorporation of Eu(III) into hydrotalcite: a TRLFS and EXAFS study. Environ. Sci. Technol. 41, 3186–3191.

Supkowski, R.M., Horrocks Jr., W.D.e.W., 2002. On the determination of water molecules, q, coordinated to europium(III) ions in solution from luminescence decay lifetimes. Inorg. Chim. Acta 340, 44–48.

Tertre, E., Berger, G., Simoni, E., Castet, S., Giffaut, E., Loubet, M., Catalette, H., 2006. Europium retention onto clay minerals from 25 to 150 °C: experimental measurements, spectroscopic features, and sorption modelling. Geochim. Cosmochim. Acta 70, 4563–4578.

Uysal, I.T., Golding, S.D., 2003. Rare earth elements fractionation in authigenic illite-smectite from late Permian clastic rocks, Bowen basin, Australia: implications for physico-chemical environments of fluids during illitization. Chem. Geol. 193, 167–179.

Venkatramu, V., Navarro-Urrios, D., Babu, P., Jayasankar, C.K., Lavìn, V., 2005. Fluorescence line narrowing spectral studies of Eu^{3+}-doped lead borate glass. J. Non-Cryst. Solids 351, 929–935.

Wright, A.O., Seltzer, M.D., Gruber, J.B., Chai, B.H.T., 1995. Site-selective spectroscopy and determination of energy levels in Eu^{3+}-doped strontium fluorophosphates. J. Appl. Phys. 78 (4), 2456–2467.

Zigan, F., Rothbauer, R., 1967. Neutronenbeugungsmessungen am Brucit. Jahrb. Mineral. Monatsh. 137–143.

Zwicky, H.U., Grambow, B., Magrabi, C., Aerne, E.T., Bradley, R., Barnes, B., Graber, T., Mohos, M., Werme, L.O., 1989. Corrosion behavior of British Magnox waste glass in pure water. Mater. Res. Soc. Symp. Proc. 127, 129–136.